Applied Physics A
Materials Science & Processing
CrossMark
Applied Physics A Materials Science & Processing

Electrospinning of silver nanoparticles loaded highly porous cellulose acetate nanofibrous membrane for treatment of dye wastewater

Ke Wang†[a] • Qian Ma†[a] • Shu-Dong Wang*[ab] • Hua Liu*[a] • Sheng-Zhong Zhang[a] • Wei Bao[c] • Ke-Qin Zhang*[b]

[a]*Jiangsu Research and Development Center of the Ecological Textile Engineering and Technology, College of Textile and Clothing, Yancheng Institute of Industry Technology, Yancheng 224005, P. R. China.*

[b]*National Engineering Laboratory for Modern Silk, College of Textile and Clothing Engineering, Soochow University, Suzhou 215123, P. R. China.*

[c]*Wuxi Entry-Exit Inspection and Quarantine Bureau, Wuxi 214001, P. R. China.*

Abstract In this paper, silver nanoparticles (NPs) were reduced form silver nitrate. Morphology and distribution of the synthesized silver NPs were characterized. In order to obtain cellulose acetate (CA) nanofibrous membrane with high effective adsorption performance to carry silver NPs for treatment of dye wastewater, different solvent systems were used to fabricate CA nanofibrous membranes with different morphologies and porous structures via electrospinning. Morphologies and structures of the obtained CA nanofibrous membranes were compared by Scanning Electron Microscopy (SEM), which showed that CA nanofibrous membrane obtained from acetone/dichloromethane (DCM) (1/2, v/v) was with

* Corresponding authors. Email address: sdwang1983@163.com (S.D. Wang), ycfylh@126.com (H. Liu) and kqzhang@sud.edu.cn (K.Q. Zhang)

† These authors contributed equally to this publication.

the highly porous structure. SEM, Energy Dispersive Spectrometry (EDS) and Fourier Transform Infrared Spectrometry (FTIR) showed that the silver NPs were effectively incorporated in the CA nanofibrous membrane and the addition of silver NPs did not damage the porous structure of the CA nanofibrous membrane. Adsorption of dye solution (rhodamine B aqueous solution) revealed that the highly porous CA nanofibrous membrane exhibited effective adsorption performance and the addition of silver NPs did not affect the adsorption of the dye. Antibacterial property of the CA nanofibrous membrane showed that the silver loaded highly porous CA nanofibrous membrane had remarkable antibacterial property when compared to the CA nanofibrous membrane without silver NPs. The silver loaded highly porous CA nanofibrous membrane could be considered as an ideal candidate for treatment of the dye wastewater.

Keywords cellulose acetate · electrospining · porous structure · dye removal · antibacterial

Introduction

Organic dyes are one of the major pollutants released into wastewater from various industries including dyeing, paper, tannery, paint, cosmetic and textile, which have caused severe water pollution because of their brilliance, non-biodegradability and toxicity even at a very low concentration.[1,2] Thus, the removal of dyes from wastewater before it is discharged is environmentally important. Membrane filtration technology has been proved to be an attractive and competitive method for dye removal due to no requirement of introducing chemicals, simplicity, high efficiency and economy.[3,4] As one of the filtration membranes, nanofiltration membranes have become increasingly popular due to their properties between those of ultrafiltration and reverse osmosis membranes, and significant advantages over reverse osmosis membranes include low operation pressure, high permeate flux, high

rejection of low molecular weight organic compounds such as divalent salts and dyes, and relatively low operating costs.[5-7] In general, separation and adsorption performance, permeability and lifetime of the membranes mainly depend on porous structure and porosity of the membranes and membrane resistance to fouling since 1) membranes with larger surface to mass ratio, lower density and pore sizes, and higher porosity exhibit higher filtration efficiency, 2) membranes with antifouling property indicate higher separation performance and longer lifetime.[8,9] Up to now, how to produce nanofiltration membranes with the above characteristics has become the subject of much attention.

Usually, nanofibrous membranes are considered as the main part of nanofiltration membranes since they can offer higher permeability due to their larger specific surface area, higher fiber aspect ratio and higher porosity.[10,11] Therefore, many studies have focused on fabrication of nanofibrous membranes via electrospinning due to it is a simple and cost effective method to produce fibrous mats with micro to nanometer fiber diameter range, controllable composition, porous structure from polymer solutions.[12-14] Electrospinning allows the functionalization of nanofibrous membranes through simply incorporation of different types of nanomaterials and/or tailoring the nanofibers' inner structures, which include core-shell, tri-layer, side-by-side structures and also NPs or pores within the nanofibers.[15-19] Often, most electrospun nanofibrous membranes with porous structures have been reported refer to nanofibrous membranes with pores between fibers rather than pores also exist on fibers, fibers in the membranes have very smooth surface. It is known that the formation of biofilm on the membrane surface and clogging of the membrane pores caused by dye molecules are two major factors in membrane fouling due to their hydrophobic nature and the lack of antimicrobial activity, which can reduce separation performance of the membranes and shorten membrane life.[20] To improve antifouling performance of the membranes, various approaches to improve membrane hydrophilic property by changing membrane surface

property or to impart antibacterial property to the membranes by using antibacterial agents have been explored. The typical methods of changing membrane surface property to hydrophilic include incorporation of inorganic additives like Si, SiO_2, ZrO_2, TiO_2 NPs, etc.,[21,22] addition of organic hydrophilic polymers like cellulose acetate phthalate (CAP), polyvinyl alcohol (PVA), polyvinylpyrrolidone (PVP), and so on,[23,24] coating with hydrophilic polymers,[25] and grafting with hydrophilic polymers or monomers.[26,27] However, these methods are relatively complicated as compared to directly use of natural hydrophilic polymer. As one kind of cellulose derivatives, CA has advantages of abundant availability, good mechanical property, high stability to most organic solvents, biodegradability, compatibility with biological systems, and most importantly, high percentage of hydroxyl groups which will bring improved antifouling performance.[28] The most widely used antibacterial agents are antibacterial NPs, in particular, noble metal and metal oxides, including silver and gold NPs, copper, zinc and titanium oxides. Among them, silver NPs are the most commonly used on account of their high surface area, chemical stability, catalytic activity and antimicrobial efficiency.[29,30]

To our knowledge, reports about electrospun CA nanofibers containing specific nanoparticles for wastewater treatment have been reported,[30-32] but research about preparation of highly porous electrospun CA absorptive nanonofibrous membrane (pores between and exist on fibers) containing silver NPs with antibacterial property and efficient separation performance for dye removal is rarely reported. Hence, in this work, we firstly synthesized colloidal silver NPs, and then the highly porous CA nanofibrous membrane loaded silver NPs was prepared by via electrospinning. We investigated the possibility of the membrane as the candidate for treatment of the dye wastewater.

Materials and methods

Materials

Silver nitrate ($AgNO_3$) (99.99wt%), PVP (PVP-K30, M_n =40 000) and CA (M_n=30 000, 39.8 wt% acetyl content) were purchased from Sigma Aldrich. Ethanol (98wt%), DCM (98wt%), acetic acid (98wt%), acetone (98wt%) were purchased from Shanghai Chemical Reagent Co. Ltd. All chemicals were used without further purification.

Synthesis of silver nanoparticles

Firstly, 1.7g PVP used as the capping agent to protect the synthesized silver NPs from agglomeration was dissolved in 10 ml ethanol and heated up to 160°C until it turned from colorless to light yellow. Then, 0.17g of $AgNO_3$ in another 10 ml ethanol was added dropwise into the above solution. The reaction was allowed to proceed at this temperature until the color of the solution turned brown, which indicates the formation of silver NPs. The silver colloidal solution was cooled down to room temperature and centrifuged at 10000rpm for 10min to collect the silver NPs. Then, the silver NPs were washed repeatedly with anhydrous ethanol and dispersed in ethanol. The concentration of silver NPs in ethanol was tested as 10g/L.

Preparation of different CA nanofibrous membranes by electrospinning

For pure CA samples, CA solutions were prepared by dissolving 17wt% CA in acetone/acetic acid (2/1, v/v), acetone/DCM (2/1, v/v) and acetone/DCM (1/2, v/v) solvent systems respectively and stirring for 3 h using magnetic stirrer. For the sample containing silver NPs, pure CA solution was prepared by dissolving 17 wt% CA in acetone/DCM (1/2, v/v) solvent system and stirring for 3 h using magnetic stirrer. Then, 5wt% silver NPs (on the basis of the weight of CA) was added into the CA solution. The blend solution was placed under sonication for 4 h. Electrospinning was carried out at an applied voltage of 17.5 kV,

tip-to-collector distance of 15 cm, and a solution feed rate of 1 $mL.h^{-1}$ at room temperature. The ambient temperature and humidity were controlled around 23°C and 70%.

Characterization of synthesized silver NPs and prepared CA nanofibrous membranes

Morphology of the synthesized silver NPs were characterized by TEM (H-7650, Hitachi) at an operating voltage of 200 kV. Samples for TEM were prepared by dropping particles dispersed in cyclohexane onto a carbon coated copper grid, which was then dried under ambient conditions prior to being introduced into the TEM chamber. Size distribution of the synthesized silver NPs was obtained by the laser particle size analyzer (ZETASIZER NANO Series, Malvern). Morphologies of the fabricated CA nanofibrous membranes with and without silver NPs were analyzed by SEM (S-4700, Hitachi), the CA nanofibrous membranes with silver NPs were also analyzed by another SEM (S-3700N, Hitachi). Samples for SEM were examined at an accelerating voltage of 15 kV. Distribution of silver NPs in the highly porous CA nanofibrous membrane was studied by EDS (S-3700N, Hitachi). Chemical structures of the highly porous CA nanofibrous membranes with and without silver NPs were investigated by FTIR (Nicolet 5700, PE Co., USA) in the range of 400-4000 $cm^{-1}$with a signal resolution of 1 $cm^{-1}$and a minimum of 16 scans. All samples were ground with potassium bromide (KBr) and pressed into pellets before testing.

Dye adsorption measurement

Adsorption capacity of the CA nanofibrous membranes with and without silver NPs was evaluated using aqueous Rhodamine B solution. Samples (60 mg) were immersed into a Rhodamine B aqueous solution (10mL, 1×10^{-6}mol/L) for 24 h at 25℃. After adsorption, the concentration of the Rhodamine B solution decreased. Optical absorption spectra of the solutions were measured an UV-visible spectrophotometer (Shimadzu UV2450, Japan). The

adsorption ratio of Rhodamine B can be calculated by formula (1).

$$Absorption\ ratio = (1 - \frac{A}{A_0}) \times 100\% \quad (1)$$

Where A_0 and A are the absorbance values before and after dye adsorption process.

Antibacterial property test

The antibacterial property of the highly porous CA nanofibrous membrane electrospun by using acetone/DCM (1/2, v/v) with and without silver NPs was tested against Gram positive S. aureus and Gram negative E. coli. The cultures were maintained in nutrient agar slopes at 4°C and sub cultured on nutrient agar plates. The concentration of isolated colonies of S. aureus and E. coli was adjusted to 1-2×10^7 CFU/ml by 0.5 Mcfarland standards. The culture was inoculated on Muller-Hinton agar plates. Nanofibrous membrane disks were placed aseptically on the Muller-Hinton agar medium which was already swabbed with the test organism. The plates were incubated at 37°C for 24 h to observe the inhibition zone. The antimicrobial efficiency of the nanofibrous membrane was tested against Gram positive S. aureus and Gram negative E. coli by using a shaking flask method according to FZ/T 73023-2006 (China). [33]

Results and discussion

Morphology and size distribution of the synthesized silver NPs

Morphology of synthesized silver NPs is illustrated in Figure 1a and b. It can be seen that silver NPs are uniformly scattered in high monodispersion and are spherical in shape. The high monodispersion of the synthesized silver NPs can be attributed to the addition of PVP, which acted as a solvent, stabilizer, reducing agent and formed a stabilizing bilayer between the silver surface and the ethanol, thus limited particles growth and hindered

agglomeration.[34,35] Despite this, mild cross-linking and agglomeration still can be noticed, this is because ethanol is a low polar solvent and the formation of weak electrical double layer.[36] The diameter distribution of the as-obtained silver NPs is displayed in Figure 1c. It can be seen that the size distribution is narrow and the average diameter of the synthesized silver NPs is 13 ± 2 nm.

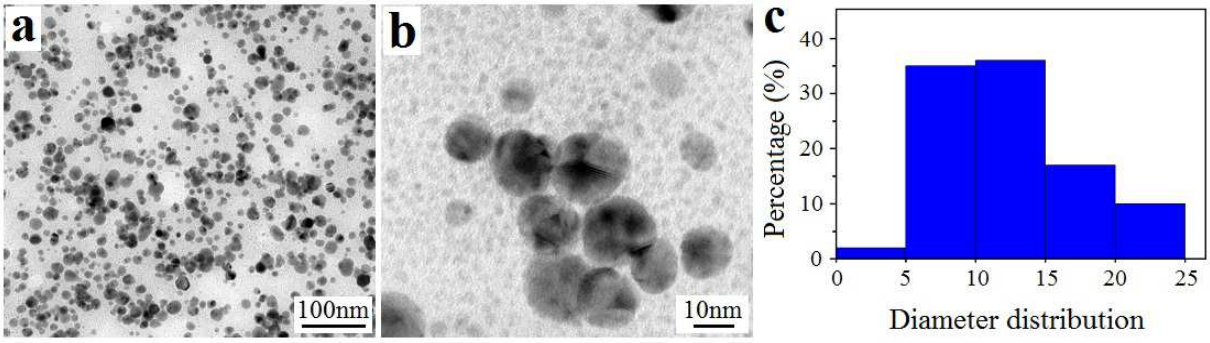

Figure 1. (a) TEM, (b) high resolution TEM images of silver NPs and (c) diameter distribution of silver NPs.

Morphology of the CA and silver loaded CA nanofibrous membranes

Morphology of the CA nanofibrous membranes fabricated by using three different solvent systems, with and without silver NPs were studied by SEM, which is shown in Figure 2 and Figure 3. From Figure 2 and Figure 3, we can find that continuous and beadless electrospun CA fibers with and without silver NPs were obtained from all solvent systems selected. From Figure 2, all CA fibers show mixture of both ribbon-like and cylindrical fiber structures. The ribbon-like/cylindrical fiber ratio increased as the solvent system changed from acetone/acetic acid (2/1, v/v) to acetone/DCM (2/1, v/v), and then acetone/DCM (1/2, v/v). This is attributed to the relatively high volatility of the used solvent systems and difference in their volatility. For the three solvents selected, DCM (boiling point (BP) = 40°C) is of the highest volatility, followed by acetone (BP=56°C) and acetic acid (BP=118.1°C), which led to the relatively

high volatility of the three used binary solvent systems. It is known that the high volatility of the used solvent system can produce ribbon-like fibers since it can bring the formation of a skin structure on the surface of the fiber, which collapses under the atmospheric pressure after the solvent evaporates rapidly from the inside of the fiber.[37,38] The different ribbon-like/cylindrical fiber ratio is caused by the volatility difference of the three used solvent systems. In particular, the ribbon-like/cylindrical fiber ratio increased as the volatility of the solvent system increased since the volatility of acetone/acetic acid (2/1, v/v, BPmix=76.7°C) < that of acetone/DCM (2/1, v/v, BPmix=51°C) < that of acetone/DCM (1/2, v/v, BPmix=45°C). In addition, compare images at higher magnification in Figure 2, other interesting morphological differences can be found. As shown in Figure 2a, there are grooves on the surface of the fibers obtained by using acetone/acetic acid (2/1, v/v). This can be attributed to the volatility difference of acetone and acetic acid. On the one hand, the relatively high volatility of acetone led to the relatively rapid evaporation of acetone, which made the surface of the fiber collapsed under the atmospheric pressure. On the other hand, the relatively low volatility of acetic acid led to slight move rather than rapid solidification of the CA polymer chains. It is because the cooperative effect of acetone and acetic acid, grooves rather than holes or pores formed on the surface of the fibers. For fibers obtained from using acetone/DCM (2/1, v/v) (Figure 2b), not only grooves but also a certain amount of holes exist on the surface of the fibers. This is because that both acetone and DCM are highly volatile solvents, especially the DCM. In solvent-rich regions, fast evaporation of solvent and rapid solidification of CA polymer chains gave rise to phase separation, which transformed into holes.[39] When the DCM/acetone ratio increased from 1/2 to 2/1 (v/v) (Figure 2c), it can be

observed that the surface of the fiber is full of grooves, holes and micropores as compared to Figure 2b. This indicates that the highly volatile DCM is responsible for the existence of micropores on the fiber surface. The higher the content of DCM in the solvent system, the more micropores were formed on the fiber surface, which in turn means nanofibrous membrane with more porous structure can be obtained. From the above comparison, we can know that CA nanofibrous membrane with more porous fiber structure can be obtained by using acetone/DCM solvent system than by using acetone/acetic acid solvent system. Furthermore, the morphology and the porous structure of the CA fibers depend on the content of DCM in the binary system. Among the selected three solvent systems, CA nanofibrous membrane obtained from acetone/DCM (1/2, v/v) is with the highest porous structure. Therefore, nanofibrous membrane obtained from acetone/DCM (1/2, v/v) was selected as the substrate to carry silver NPs. Figure 3 shows the silver loaded CA nanofibrous membrane obtained by using acetone/DCM (1/2, v/v). Samples used for images of Figure 3a, b, c were coated with gold, while samples used for images of Figure 3d, e, f were not coated with gold. Compare Figure 3a, b, c with Figure 2c, the morphology of the silver loaded nanofibers remained same, the addition of the silver NPs didn't result in beaded fibers or damage the porous structure of the CA nanofibrous membrane. As Figure 3d, e, f shows, the silver NPs were successfully incorporated into/on the CA fibers. Distribution of silver NPs in/on the fibers was also confirmed by EDS analysis (Figure 4). As can be seen from Figure 4b, the weight of silver NPs accounts for 4.063wt%, almost as same as the weight of silver NPs had been added in. It shows that most of the silver NPs dispersed on the surface of the CA fibers. The weight of silver NPs was tested less than 5wt% on account of the embedment of a small

amount of silver NPs in the CA fibers. Homogenous distribution of yellow dots in Figure 4c indicates that silver NPs were well introduced with visibly widely dispersion. More concentrated distribution of silver NPs or bigger silver NPs in some areas reflected in yellow dots with higher visibility.

With respect to the fiber size, acetone/acetic acid (2/1, v/v) produced fiber with the lowest average diameter of 2.03μm (Figure 2a). Using solvent system with higher volatility, acetone/DCM (2/1, v/v) yielded fibers with an average width of 4.61μm (Figure 2b) and fibers with an average width of 4.92μm (Figure 2c) were obtained by acetone/DCM (1/2, v/v). The increase in average fiber diameter is observed as the volatility of the three used solvent systems gradually increases, this is because that the faster evaporation of the solvent system decreased the time left for the stretch of the droplet.[36] Compare Figure 2c with Figure 3, the average diameter of fibers containing silver NPs produced by acetone/DCM (1/2, v/v) decreases to 3.78μm due to the decrease in the viscosity of the electrospinning solution when silver colloidal solution were added in.

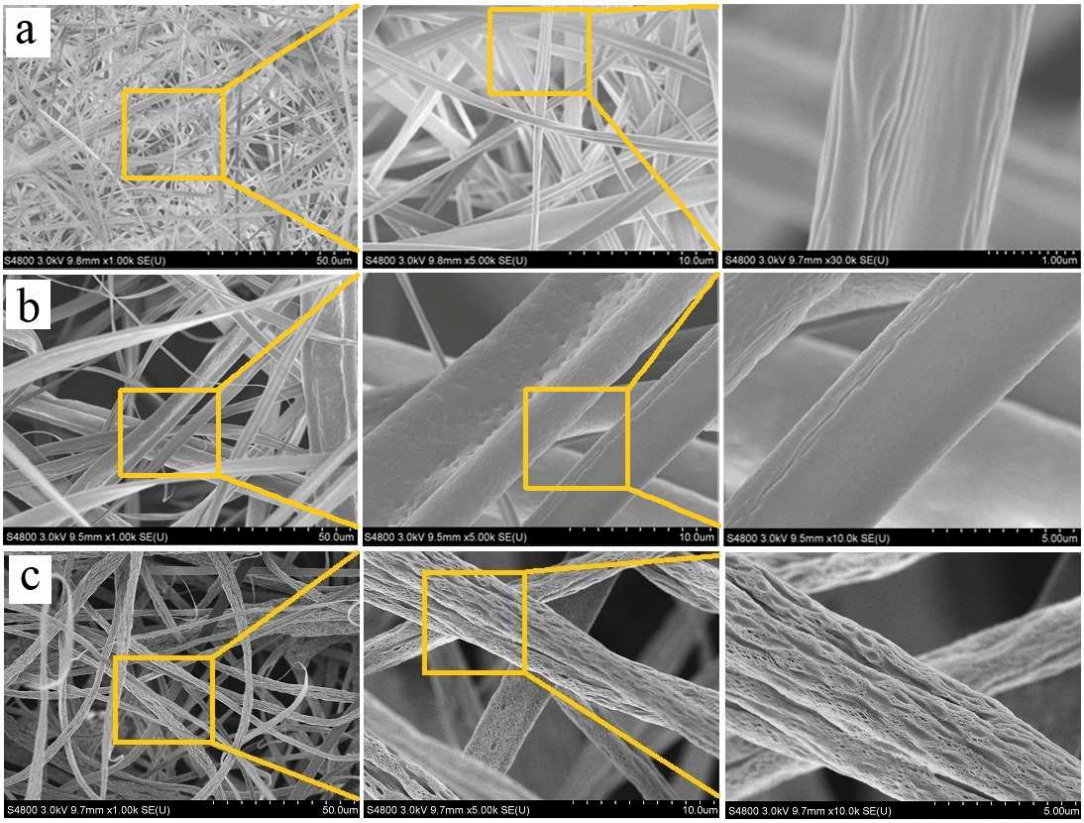

Figure 2. SEM images of CA nanofibrous membranes prepared by using (a) acetone/acetic acid (2/1, v/v), (b) acetone/DCM (2/1, v/v), (c) acetone/DCM (1/2, v/v).

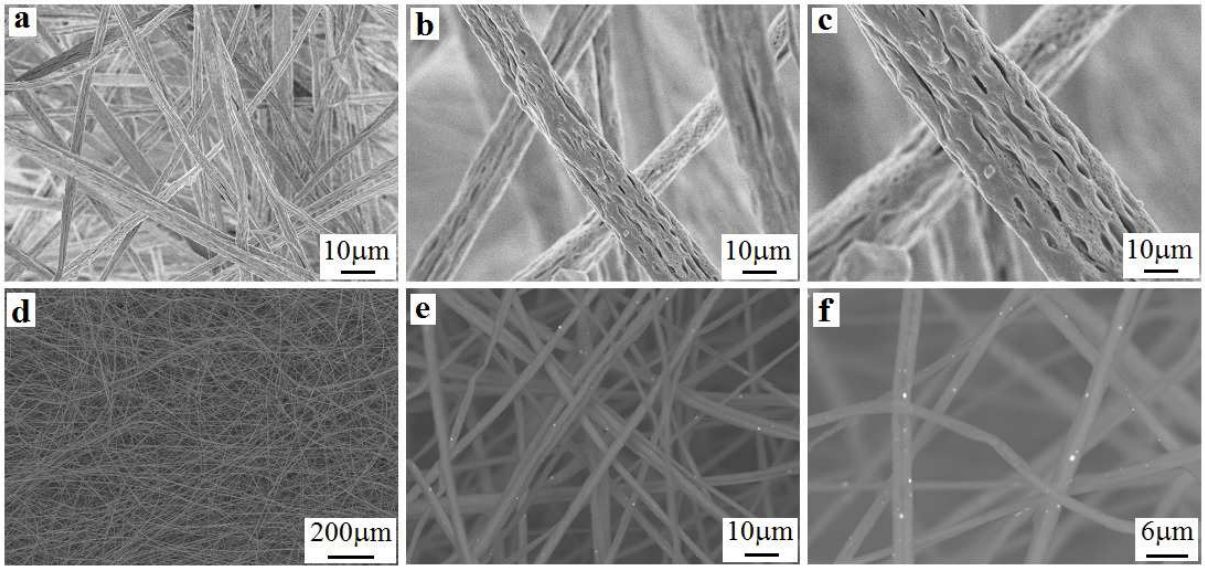

Figure 3. SEM (coated with gold(a)-(c) and without coated with gold (d)-(f)) images of CA nanofibrous membrane (using acetone/DCM (1/2, v/v)) containing silver NPs.

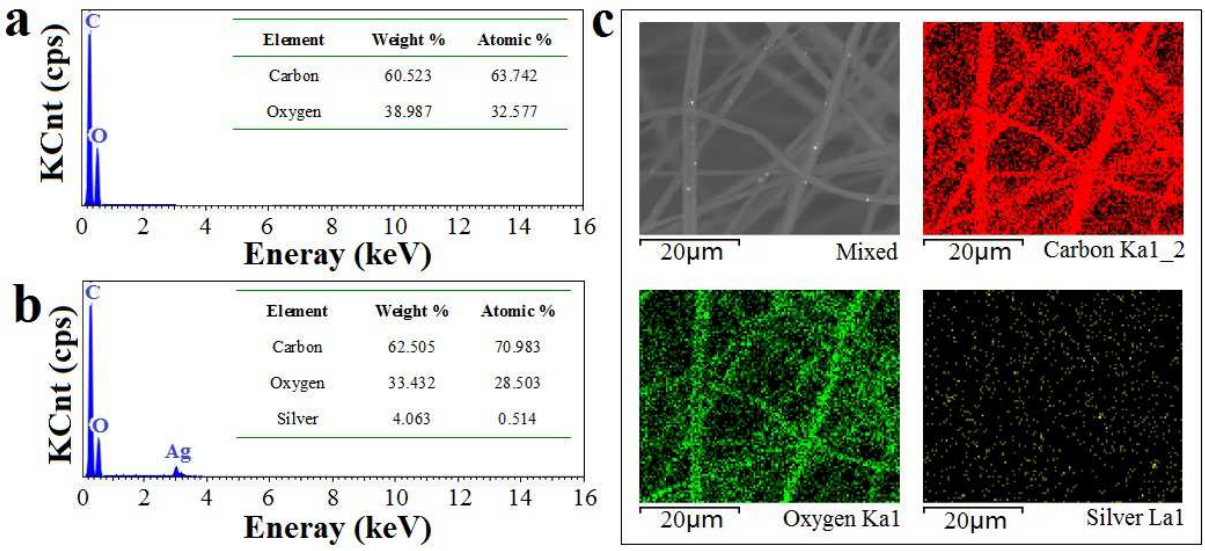

Figure 4. EDS spectrum of (a) pure highly porous CA nanofibrous membrane and (b) highly porous CA nanofibrous membrane containing silver NPs (electrospun by using acetone/DCM (1/2, v/v)) and (c) mapping-scan of highly porous CA nanofibrous membrane containing silver NPs (electrospun by using acetone/DCM (1/2, v/v)).

Chemical structure of the highly porous CA and silver loaded CA nanofibrous membranes

The functional groups present in the samples and the interaction between silver and CA were analyzed by FTIR. As shown in Figure 5, the main characteristics peaks of CA at 3500cm^{-1}, 2960cm^{-1}, 1750cm^{-1}, 1250cm^{-1} and 1050cm^{-1} are related to O-H, υ(C-H)(CH3), υ(C=O) carbonyl, C-O group acetyl and υ(C-O-C), respectively.[40] After silver NPs incorporation, FTIR spectra of the highly porous CA nanofibrous membrane with silver NPs was almost same as that of the pure highly porous CA nanofibrous membrane except the intensity of the peaks at the wave number of 1050cm^{-1} increased, which not only confirms the addition of silver NPs but also indicates that the introduction of silver NPs did not affect the hydrophilic property of CA and functional groups of CA interacted with silver NPs.

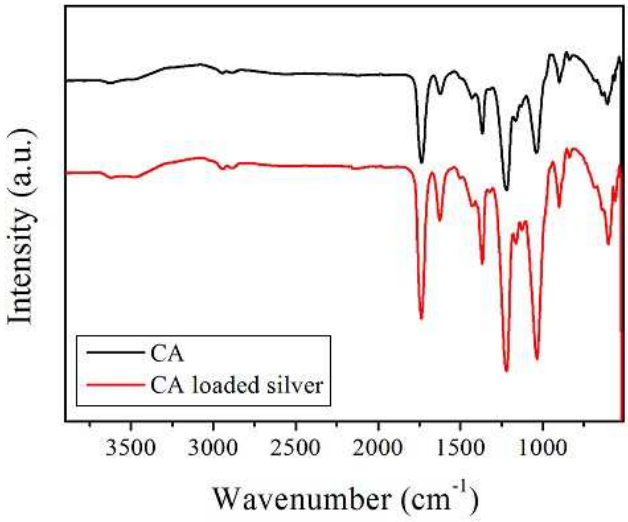

Figure 5. FTIR spectra of pure porous CA nanofibrous membrane and porous CA nanofibrous membrane containing silver NPs.

Dye adsorption

Adsorption performance of all CA nanofibrous membranes with and without silver NPs was compared by investigating the change in the absorbance at λ_{max} = 551nm of Rhodamine B solutions containing different CA samples with the reaction time, by measuring the concentration of Rhodamine B in the solution after underwent adsorption and by observing the color change of Rhodamine B solution. As shown in Figure 6, the absorbance at λ_{max} = 551nm of Rhodamine B solutions containing different CA samples decreased to various extents with the reaction time. The decrease in absorbance is due to the adsorption of the Rhodamine B. Therefore, the adsorption ratio can be determined by measuring the absorbance value of the Rhodamine B solution at λ_{max} = 551nm. The lower absorbance value indicates more adsorption of Rhodamine B. From Figure 7a, absorbance values of solutions containing CA nanofibrous membranes obtained from acetone/acetic acid (2/1, v/v), acetone/DCM (2/1, v/v), acetone/DCM (1/2, v/v) and acetone/DCM (1/2, v/v) loaded with silver NPs are 0.106, 0.1, 0.095 and 0.092. Accordingly, their adsorption ratios of Rhodamine B are calculated as 32.9%, 36.7%, 39.9% and 41.7%, respectively (shown in Figure 8). From Figure 7b, Rhodamine B decolored to varying degrees due to difference in adsorption performance of different CA samples. It can be seen that whether there are micropores on the fiber surface or not, adsorption of Rhodamine B occurred for all CA samples. This is because CA's good

hydrophilic property and the superior properties of nanofibrous membranes over other kinds of membranes, including large surface area to volume ratio, higher fiber aspect ratio and high porosity, which allow greater surface adsorption of contaminants from water. Regardless of this, amount and distribution of micropores on fiber surfaces made a difference on adsorption capability of different CA nanofibrous membranes. Evidently, CA nanofibrous membrane obtained from acetone/DCM (1/2, v/v) shows the best adsorption property, with the adsorption ratio increased from 32.9% to 39.9% and the color changed from hot pink to almost transparent as the amount and distribution of micropores on fiber surfaces increased to maximum. Therefore, it is the best candidate to load silver NPs. The results reveal that CA nanofibrous membranes can promise certain adsorption ability and micropores on fiber surfaces can help to improve adsorption ability of CA nanofibrous membranes. In brief, CA nanofibrous membrane with a more porous structure and a higher porosity implies a better adsorption performance. It also can be seen that the adsorption ratio before and after silver incorporation are 39.9% and 41.7%, together with the Rhodamine B solution decolored more thoroughly, which clearly shows the adsorption performance was slightly improved rather than reduced with the addition of silver NPs. This is probably because the more fluffy structure resulted from mildly decreased viscosity of solution caused by the addition colloidal silver NPs.

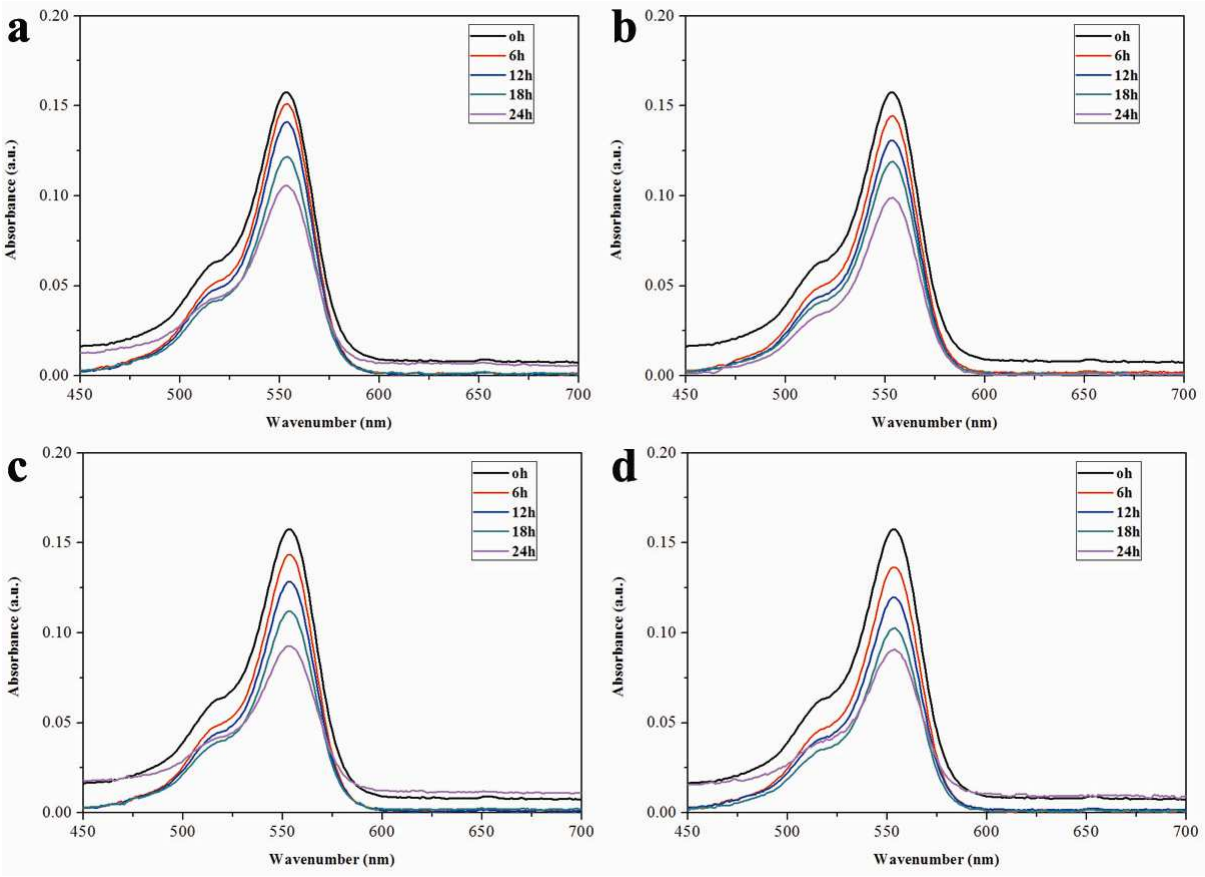

Figure 6. Change in the absorbance at λ_{max}=551nm of Rhodamine B solution with reaction time absorbed by CA nanofibers fabricated by using (a) acetone/acetic acid (2/1, v/v), (b) acetone/DCM (2/1, v/v), (c) acetone/DCM (1/2, v/v) and (d) acetone/DCM (1/2, v/v) loaded with silver NPs.

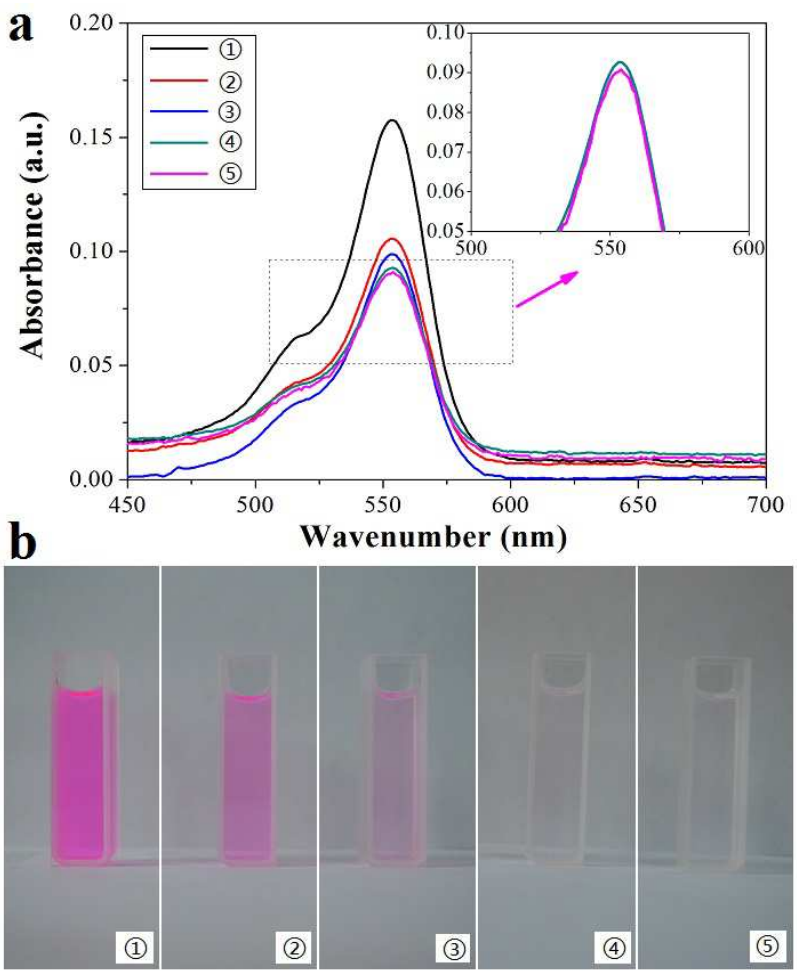

Figure 7. UV-vis spectra (a) and color change (b) of the dye removal experiment. ① initial Rhodamine B solution, ② solutions adsorbed by CA nanofibers fabricated by using acetone/acetic acid (2/1, v/v), ③ acetone/DCM (2/1, v/v), ④ acetone/DCM (1/2, v/v) and ⑤ acetone/DCM (1/2, v/v) loaded with silver NPs.

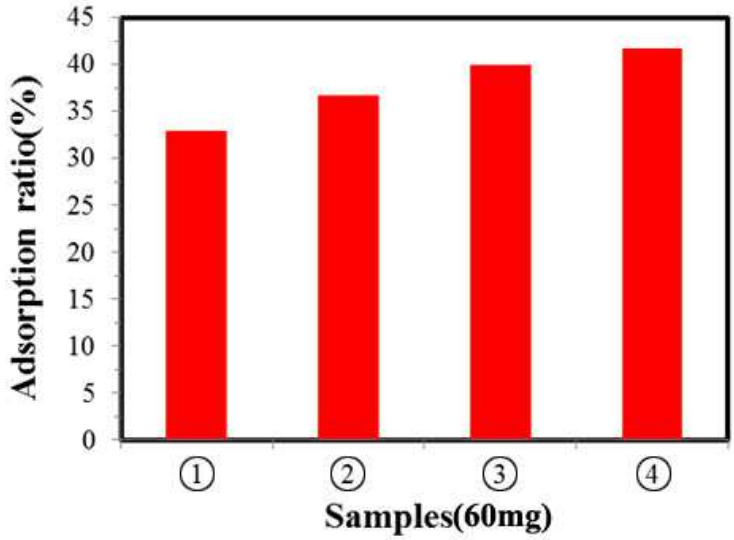

Figure 8. Adsorption ratio of CA nanofibrous membranes (60mg) prepared by using ① acetone/acetic acid (2/1, v/v), ② acetone/DCM (2/1, v/v), ③ acetone/DCM (1/2, v/v) and ④ acetone/DCM (1/2, v/v) loaded with silver NPs.

Antibacterial activity of highly porous CA adsorptive nanofibrous membrane loaded silver NPs

Antibacterial property of highly porous CA nanofibrous membrane loaded silver NPs against Gram positive S. aureus and Gram negative E. coli under normal lighting condition were investigated by means of Kirby Bauer technique. The pure highly porous CA nanofibrous membrane was used as a control. Five samples in each group were tested to ensure the effectiveness of the results. As shown in Figure 9, no detectable inhibition zones can be seen for pure CA samples. By contrast, significant zones against both microorganisms can be observed for silver NPs loaded CA samples, with the average diameter of the inhibition zone against S. aureus is 10.8±0.9 mm and that against E. aureus is 8.5±0.7 mm. We also investigated the antibacterial efficiency (Figure 10), it could be found that both the reduction rate of the Gram positive S. aureus and Gram negative E. coli are higher than 90%.

Futhermore, the reduction rate of the antibacterial efficiency has only decreased a litter within 5 cycles. The results further confirm the successful incorporation of silver NPs and show that the highly porous CA nanofibrous membrane containing silver NPs has effective antibacterial property.

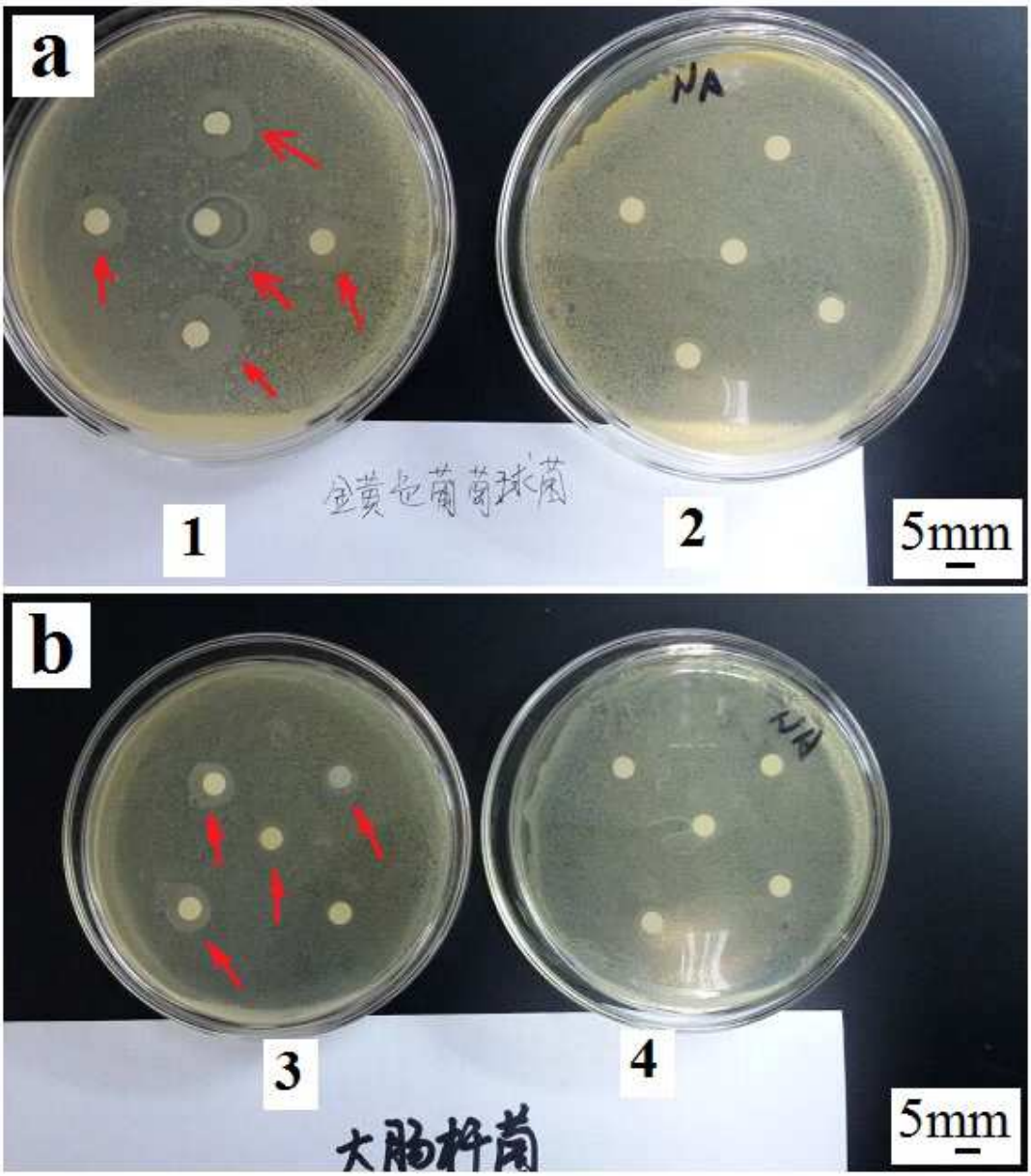

Figure 9. Antibacterial tests of S. aureus (a) and E. coli (b). 1 and 3 are highly porous CA nanofibrous membrane containing silver NPs, 2 and 4 are pure highly porous CA nanofibrous membrane

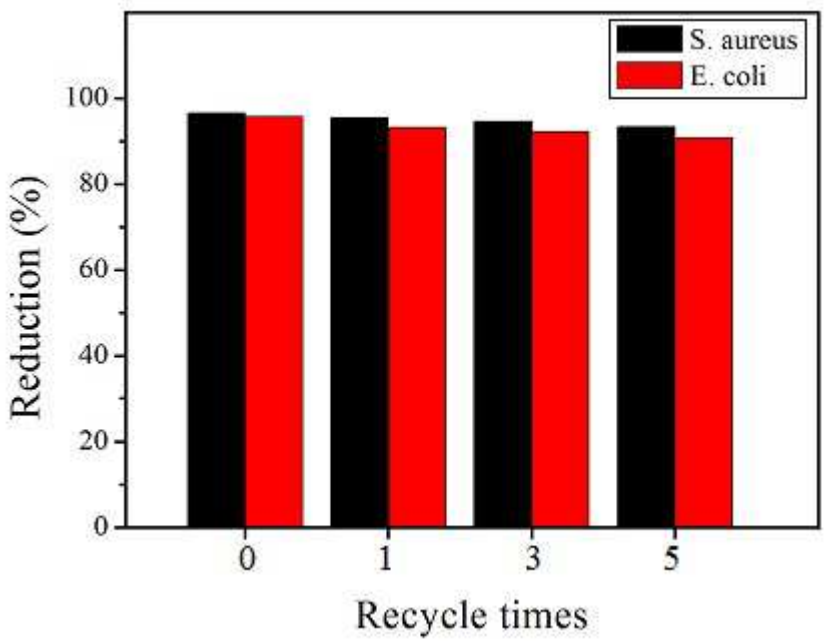

Figure 10. Antibacterial efficiency of the the nnofibrous membrane containing silver NPs and recycle test of the antibacterial efficiency.

Conclusion

Silver NPs were reduced from silver nitrate, and the TEM results show that the synthesized silver NPs were in small diameter and in high monodispersion. Bead-free electrospun CA nanofibrous membranes were successfully prepared by the selected three different solvent systems. However, the volatility difference of the selected solvent systems can greatly affect the morphologies and structures of the as obtained CA nanofibrous membranes. SEM results showed that the higher the volatility of the solvent system, the more porous structure and the higher ratio of ribbon-like fibers the yielded CA nanofibrous membrane had. Highly porous CA nanofibrous membrane can be obtained by using acetone/DCM (1/2, v/v) and it was selected to carry silver NPs. EDS results showed that silver NPs were successfully introduced into the highly porous CA nanofibrous membrane with homogenous distribution. FTIR results showed that the introduction of silver NPs did not affect the hydrophilic property of CA and

functional groups of CA interacted with silver NPs. Adsorption test results showed that membrane with higher porous structure can offer better dye adsorption ability, the highly porous CA nanofibrous membrane exhibited effective adsorption performance and the addition of silver NPs didn't affect the adsorption of the dye. Antibacterial test against Gram positive S. aureus and Gram negative E. coli showed that the highly porous CA adsorptive nanofibrous membrane containing silver NPs had effective antibacterial property. The above results indicated that the highly porous CA adsorptive nanofibrous membrane loaded silver NPs could be very promising in treatment for dye adsorption.

Acknowledgements

This research was financially supported by the Natural Science Foundation of Jiangsu Province, China (BK20131222). The authors are also grateful for Qinglan Project of Educational Department of Jiangsu Province, China (QLCG2012). This research was also financially supported by the project supported by Scientific Research Fund of Yancheng Institute of Industry Technology (ygy1409) and Science and Technology Planning Project of Jiangsu Entry-Exit Inspection and Quarantine Bureau (2015KJ18).

References

(1) Gupta, V. K.; Suhas. Application of low-cost adsorbents for dye removal-A review. *Journal of Environmental Management* **2009**, 90, 2313.

(2) Kumar, B. M. P.; Karikkat, S.; Krishnac, R. H.; Udayashankarab, T. H.; Shivaprasada, K. H.; Nagabhushanac, B. M. Synthesis, Characterization of Nano MnO_2 and its Adsorption Characteristics over an Azo Dye. *Research and Reviews: Journal of Material Sciences* **2014**, 2, 27.

(3) Amini, M.; Arami,M.; Mahmoodi, N. M.; Akbari, A. Dye removal from colored textile wastewater

using acrylic grafted nanomembrane. *Desalination* **2011**, 267, 107.

(4) Ma, S.; Meng, J. Q.; Li, J. H.; Zhang, Y. F.; Ni, L. (2014) Synthesis of catalytic polypropylene membranes enabling visible-light-driven photocatalytic degradation of dyes in water. *J. Membr. Sci.* **2014**, 453, 221.

(5) Mondal, S. Methods of Dye Removal from Dye House Effluent-An Overview. *Environ. Eng. Sci.* **2008**, 25, 383.

(6) Zhong, P. S.; Widjojo, N.; Chung, T. S.; Weber, M.; Maletzko, C. Positively charged nanofiltration (NF) membranes via UV grafting on sulfonated polyphenylenesulfone (sPPSU) for effective removal of textile dyes from wastewater. *J. Membr. Sci.* **2012** 417, 52.

(7) Huang, J.; Zhang, K. S. The high flux poly (m-phenylene isophthalamide) nanofiltration membrane for dye purification and desalination. *Desalination* **2011**, 282, 19.

(8) Hegde, C.; Isloor, A. M.; Ganesh, B. M.; Ismail, F. A.; Abdullah, M. S.; Ng, B. C. Performance of PS/PIMA/ PPEES nanofiltration membranes before and after alkali treatment for filtration of $CaCl_2$ and NaCl. *Nano Hybrids* **2012**, 1, 99.

(9) Guillen, G. R.; Farrell, T. P.; Kaner, R. B.; Hoek, E. M. V. Pore-structure, hydrophilicity, and particle filtration characteristics of polyaniline–polysulfone ultrafiltration membranes. *J. Mater. Chem.* **2010**, 20, 4621

(10) Wang, H.; Zheng, G. F.; Wang, X.; Sun, D. H. Study on the air filtration performance of nanofibrous membranes compared with conventional fibrous filters. *Proceedings of the 2010 5th IEEE International Conference on Nano/Micro Engineered and Molecular Systems* **2010**, 387.

(11) Fuenmayor, C. A.; Lemma, S. M.; Mannino, S.; Mimmo, T.; Scampicchio, M. Filtration of apple juice by nylon nanofibrous membranes. *J. Food Eng.* **2014**, 122, 110.

(12) Li, X. H.; Yang, W. M.; Li, H.Y.; Wang, Y.; Bubakir, M. M.; Ding, Y. M.; Zhang, Y. C. Water filtration properties of novel composite membranes combining solution electrospinning and needleless melt electrospinning methods. *J. Appl. Polym. Sci.* **2015**, 41601, 1.

(13) Cho, B. M.; Nam, Y. S.; Cheon, J. Y.; Park, W. H. Residual charge and filtration efficiency of polycarbonate fibrous membranes prepared by electrospinning. *J. Appl. Polym. Sci.* **2015**, 132, 1.

(14) Makaremi, M.; Silva, R. T. D.; Pasbakhsh, P. Electrospun nanofibrous membranes of polyacrylonitrile/halloysite with superior water filtration ability. *J. Phys. Chem. C* **2015**, 119, 7949.

(15) Pant, H. R.; Pandeya, D. R. Photocatalytic and antibacterial properties of a TiO_2/nylon-6 electrospun nanocomposite mat containing silver nanoparticles. *J. Hazard. Mater.* **2011**, 189, 465.

(16) Pant, B.; Pant, H. R. Characterization and antibacterial properties of Ag NPs loaded nylon-6 nanocomposite prepared by one-step electrospinning process. *Colloid. Surf. A Physicochem. Eng. Asp.* **2012**, 395, 94.

(17) Yu, D. G.; White, K.; Chatterton, N.; Li, Y.; Li, L. L.; Wang, X. Structural lipid nanoparticles self-assembled from electrospun core–shell polymeric nanocomposites. *RSC. Adv.* **2015**, 5, 9462.

(18) Gu, Z. Z.; Chen, L. Y.; Duan, B. H.; Luo, Q.; Liu, J.; Duan, C. Y. Synthesis of Au@UiO-66(NH_2) structures by small molecule-assisted nucleation for plasmonenhanced photocatalytic activity. *Chem. Commun.* **2015**, 51, 4623.

(19) Yu, D. G.; Li, X. Y.; Wang, X.; Yang, J. H.; Annie Bligh, S. W.; Williams, G. R. Nanofibers fabricated using triaxial electrospinning as zero order drug delivery systems. *ACS Appl. Mater. Interfaces.* **2015**, 7, 18891.

(20) Yun, M. A.; Yeon, K. M.; Yeon, K.; Park, J. S.; Lee, C. H.; Chun, J.; Lim, D. J. Characterization of

biofilm structure and its effect on membrane permeability in MBR for dye wastewater treatment. *Water Res.* **2006**, 40, 45.

(21) Madaeni, S. S.; Ghaemi, N. Characterization of self-cleaning RO membranes coated with TiO_2 particles under UV irradiation. *J. Membr. Sci.* **2007**, 303, 221.

(22) Khow, S.; Mitra, S.; Fabrication and characterization of carbon nanotubes immobilized in porous polymeric membranes. *J. Mater. Chem.* **2009**, 19, 3713.

(23) Yoo, J. E.; Kim, J. H.; Kim, Y. Novel ultrafiltration membranes prepared from the new miscible blends of polysulfone with poly(1-vinylpyrrolidoneco-styrene) copolymers. *J. Membr. Sci.* **2003**, 216, 95.

(24) Rahimpour, A.; Madaeni, S. S. Polyethersulfone, (PES)/cellulose acetate phthalate (CAP) blend ultrafiltration membranes: preparation, morphology, performance and anti-fouling properties. *J. Membr. Sci.* **2007**, 305, 299.

(25) Kim, K. J.; Chowdhury, G.; Matsuura, T. Low pressure reverse osmosis performance of sulfonated poly(2, 6-dimethyl-1, 4-phenylene oxide) thin film composite membranes: effect of coating conditions and molecular weight of polymer. *J. Membr. Sci.* **2000**, 179,43

(26) Akbari, A.; Desclaux, S.; Rouch, J. C.; Aptel, P.; Remigy, J. C. New UV-photografted nanofiltration membranes for the treatment of colored textile dye effluents. *J. Membr. Sci.* **2006**, 286, 342.

(27) Bequet, S.; Abenoza, T.; Aptel, P. New composite membrane for water softening. *Desalination* **2000**, 131, 299.

(28) Wang, S. D.; Ma, Q.; Liu, H.; Wang, K.; Ling, L.Z.; Zhang, K. Q. Robust electrospinning cellulose acetate@TiO_2 ultrafine fibers for dyeing water treatment by photocatalytic reactions. *RSC. Adv.* **2015**, 5, 40521.

(29) Gouda, M.; Hebeish , A. A.; Al-Omair, M. A. Development of silver-containing nanocellulosics for

effective water disinfection. *Cellulose* **2014**, 21, 1965.

(30) Jang, K. H.; Kang, Y. O. Functional cellulose-based nanofibers with catalytic activity: Effect of Ag content and Ag phase. *Int. J. Biolo. Macromol.* **2014**, 67, 394.

(31) Zhang, L.F.; Menkhaus, T. J.; Fong, H. Fabrication and bioseparation studies of adsorptive membranes/felts made from electrospun cellulose acetate nanofibers. *J. Membr. Sci.* **2008**, 319, 176.

(32) Jang, K.H.; Kang, Y. O. Photocatalytic activities of cellulose-based nanofibers with different silver phases: Silver ions and nanoparticles. *Carbohydr. Polym.* **2014**, 102, 956.

(33) Qu C.X.; Wang, S.D. Macro-micro structure, antibacterial activity, and physico-mechanical properties of the mulberry bast fibers. *Fiber. Polym.* 2011, 12, 471.

(34) Zhao, T.; Sun, R.; Size-controlled preparation of silver nanoparticles by a modified polyol method. *Colloid. Surf. A Physicochem. Eng. Asp.* **2010**, 366, 197.

(35) Le, A. T.; Le, T. T. Powerful colloidal silver nanoparticles for the prevention of gastrointestinal bacterial infections. *Adv. Nat. Sci. Nanosci. Nanotechnol.* **2012**, 3, 1.

(36) Tilaki, R. M.; Irajizad, A. Stability, size and optical properties of silver nanoparticles prepared by laser ablation in different carrier media. *Appl. Phys. A* **2006**, 84,215.

(37) Rodrı´guez, K.; Gatenholm, P.; Electrospinning cellulosic nanofibers for biomedical applications: structure and in vitro biocompatibility. *Cellulose* **2012**, 19, 1583.

(38) Koombhongse, S.; Liu, W.; Reneker, D. H. Flat polymer ribbons and other shapes by electrospinning. *J. Polym. Sci. Part B* **2001**, 39, 2598.

(39) Celebioglu, A; Uyar, T. Electrospun porous cellulose acetate fibers from volatile solvent mixture. *Mater. Lett.* **2011**, 65, 2291.

(40) Kendouli, S.; Khalfallah, O. Modification of cellulose acetate nanofibers with PVP/Ag addition. *Mat.*

Sci. Semicon. Proc. **2014**, 28, 13.